Journal of Cleaner Production 252 (2020) 119887

Contents lists available at ScienceDirect

Journal of Cleaner Production

journal homepage: www.elsevier.com/locate/jclepro

Spatiotemporal patterns of global air pollution: A multi-scale landscape analysis based on dust and sea-salt removed $PM_{2.5}$ data

Huanbi Yue [a, b], Qingxu Huang [a, b], Chunyang He [a, b, *], Xiaoling Zhang [c, d], Zihang Fang [a, b]

[a] Center for Human-Environment System Sustainability (CHESS), State Key Laboratory of Earth Surface Processes and Resource Ecology (ESPRE), Beijing Normal University, 19 Xinjiekouwai Street, Haidian District, Beijing, 100875, China
[b] School of Natural Resources, Faculty of Geographical Science, Beijing Normal University, 19 Xinjiekouwai Street, Haidian District, Beijing, 100875, China
[c] Urban Research Group, Department of Public Policy, City University of Hong Kong, Tat Chee Avenue, Kowloon, Hong Kong, 999077, China
[d] Shenzhen Research Institute, City University of Hong Kong, 8 Yuexing 1st Road, Nanshan District, Shenzhen, 518057, China

ARTICLE INFO

Article history:
Received 28 February 2019
Received in revised form
12 December 2019
Accepted 26 December 2019
Available online 26 December 2019

Handling editor: Giovanni Baiocchi

Keywords:
$PM_{2.5}$ pollution
Anthropogenic activities
Landscape metric
Income level
Public health
Urban sustainability

ABSTRACT

Spatiotemporal patterns of global air pollution are of great significance to environmental management and public health. Studies have revealed the changes in the concentration of dust and sea-salt removed fine particulate matter ($PM_{2.5}$) pollution (DSRPP). However, the spatial characteristics of DSRPP on multiple scales remain unclear. Therefore, we combined the latest global estimates of the $PM_{2.5}$ dataset and landscape metrics to investigate the spatiotemporal patterns of DSRPP across global and national scales from 2000 to 2016. We found that the area of DSRPP increased from 1,146,800 km^2 to 3,929,800 km^2 between 2000 and 2016, a factor of 2.43. The DSRPP became more structurally fragmented and geometrically complex, with the patch density and the landscape shape index of DSRPP increasing by 133.3% and 24.5%, respectively. More than 90% of the DSRPP were concentrated in the middle income countries, especially in India and China. Specifically, the DSRPP in China exhibited a sprawling process before 2007 but a dissipating process after 2007 under the great efforts of the Chinese government in mitigating air pollution, while DSRPP in India remained an aggregation trend. The potential threat to public health posed by the DSRPP increased over time. Populations living in the areas with the DSRPP increased by 141.2% from 2000 to 2016 due to the deterioration of air quality and demographic change. Thus, we suggest that effective actions should be taken to control the main sources of anthropogenic emissions and mitigate the negative effects of DSRPP on public health in the future, especially in the middle income countries such as China and India.

1. Introduction

Dust and sea-salt removed fine particulate matter ($PM_{2.5}$) pollution (DSRPP) is defined as the presence of $PM_{2.5}$ components without dust and sea-salt in the atmosphere at a sufficient concentration, for a sufficient time, and under circumstances such that it interferes with the comfort, health, or welfare of people or the environment (ISO, 1994; Kaiser, 2005). DSRPP includes such constituents as sulfate, nitrate, ammonium, and carbonaceous aerosols (van Donkelaar et al., 2016). Investigating the DSRPP is of great significance for public health and sustainable development. First, DSRPP can be used to approximate anthropogenic $PM_{2.5}$ pollution, which is highly relevant to human activities (Evans et al., 2013). Furthermore, DSRPP has notable effects on human health (Wu et al., 2013; Burnett et al., 2014). Hence, DSRPP is directly related to United Nations' Sustainable Development Goal (SDG), i.e., SDG3 (good health and well-being) and SDG11 (sustainable cities and communities) (WHO, 2016).

Several studies investigated the impacts of DSRPP on public health. At the global scale, Evans et al. (2013) found that DSRPP was attributable to 8.0%, 12.8% and 9.4% for the cardiopulmonary disease, lung cancer and ischemic heart disease, respectively. Lelieveld et al. (2015) assessed the premature mortality attributable to $PM_{2.5}$ from seven emission sources in 2010 and found that more than 80% of the global total deaths were related to the anthropogenic sources. At the continental scale, Lacey et al. (2017) estimated that 13,000 premature deaths were related to anthropogenic emissions

* Corresponding author. at: State Key Laboratory of Earth Surface Processes and Resource Ecology, Beijing Normal University, 19 Xinjiekouwai Street, Beijing, 100875, China.
E-mail address: hcy@bnu.edu.cn (C. He).

https://doi.org/10.1016/j.jclepro.2019.119887
0959-6526/

in Africa, and the largest contribution came from residential activity. At the national scale, Crouse et al. (2016) simulated the risk related to $PM_{2.5}$ in south Canada, and the results indicated the components of DSRPP (e.g. sulfate, organic mass and ammonia) have higher toxicity than dust. Therefore, understanding the spatiotemporal patterns of DSRPP is important in making decisions to mitigate pollutant emissions and secure public health.

Researchers have studied the changes in DSRPP concentrations on multiple scales. At the global scale, Philip et al. (2014) analyzed the dynamics of DSRPP concentrations between 2004 and 2008 by combining the remotely sensed aerosol optical depth (AOD) and the Goddard Earth Observation System chemical transport model (GEOS-chem). At the national scale, Crouse et al. (2016) analyzed the changes in DSRPP concentrations in southern Canada from 2001 to 2010 by combining the AOD and GEOS-chem model. At the local scale, Cheng et al. (2016) analyzed DSRPP concentrations in forty-five global megacities for the year 2013. However, most studies mainly focused on changes in DSRPP concentrations, while changes in the spatiotemporal patterns of DSRPP have not yet been adequately evaluated.

Landscape metrics can be used to delineate the spatiotemporal patterns of DSRPP. Landscape metrics quantify the spatial characteristics of landscape elements and have been used widely in geographical and ecological research (Turner and Gardner, 2015). Previous researchers have used landscape metrics to quantify the spatiotemporal patterns of forest cover, impervious surfaces, and green space (Remmel and Csillag, 2003; Buyantuyev et al., 2010; Qian et al., 2015), and uncovered their relationship with the urban heat island and water quality (Lee et al., 2009; Zhou et al., 2011; Weber et al., 2014). Recent researchers also used landscape metrics to analyze the spatiotemporal changes in $PM_{2.5}$ pollution (Liu et al., 2017a), and found that the spatial shape of $PM_{2.5}$ pollution is closely related to the urban form (Borrego et al., 2006), industrial emission sources (Li et al., 2016), agricultural emission sources (Zhang et al., 2017a), and wind speed change (Zhang et al., 2016). Therefore, the spatiotemporal patterns of DSRPP based on the landscape metrics can enrich our understanding of the relationship between the pattern and the process of DSRPP.

The most recently published dataset of Global Estimates of Fine Particulate Matter (GEFPM) is an important data source for investigating the spatiotemporal patterns of DSRPP on multiple scales (van Donkelaar et al., 2016). First, the dataset is highly accurate because it was further calibrated using the GEOS-chem model and *in situ* monitoring data. Second, the dataset provides annually updated information for the period from 1998 to 2016. Third, the dataset provides all components $PM_{2.5}$ concentrations, as well as the dust and sea-salt removed $PM_{2.5}$ concentrations. Therefore, the GEFPM dataset enables the specific analysis of the spatiotemporal patterns of DSRPP to be made. This dataset has been successfully used in relevant studies in recent years (Han et al., 2017a; Li et al., 2017; Cao et al., 2018). Against this background, this study is the first-ever attempt to conduct a comprehensive evaluation of spatiotemporal patterns of DSRPP using rich data across space and time based on a multi-scale landscape analysis.

In this context, our objective was to analyze the spatiotemporal patterns of global DSRPP between 2000 and 2016, and further discuss the drivers and potential health impacts. We first quantified the DSRPP spatiotemporal patterns at the global and national scales between 2000 and 2016 using landscape metrics. Then, we explored the relationship between income per capita and DSRPP at the national scale. Finally, we discussed the potential threats to public health posed by DSRPP. Our results are helpful for setting policy for pollution control and understanding the influence of global air pollution on public health.

2. Data

Dust and sea-salt removed $PM_{2.5}$ concentrations were obtained from the GEFPM dataset (V4.GL.02) published by the Dalhousie University's Atmospheric Composition Analysis Group (http://fizz.phys.dal.ca/~atmos/; last accessed on December 4, 2018). Different from a previous version of this dataset (V3.01) which used a three-year average to reduce noise, this new dataset contains gridded records of global annual average $PM_{2.5}$ concentrations as well as dust and sea-salt removed $PM_{2.5}$ concentrations from 1998 to 2016 at a spatial resolution of 0.1° (approximately 10 km) without the sliding average method (van Donkelaar et al., 2015, 2016). In this study, we used the annual average dust and sea-salt removed $PM_{2.5}$ concentrations from 2000 to 2016 (Appendix Figure A1). In addition, although the dataset is calibrated by ground-based measurements of $PM_{2.5}$, most of the measured data were from the United States and Europe during 2008–2013. Under this background, we further validated the data using monitoring data in China and India. The correlation analysis showed the GEFPM dataset highly corresponded with monitoring data in India and China, which indicated the accuracy of this dataset could support our analysis (Appendix Figure A2).

The population data used in this study were obtained from the History Database of the Global Environment (HYDE3.2) published by the Netherlands Environmental Assessment Agency (ftp://ftp.pbl.nl/hyde; last accessed on December 4, 2018). This dataset contains the gridded population at a global scale between 2000 and 2016, with a spatial resolution of 0.083° (approximately 10 km) (Goldewijk et al., 2016). The country-level income data and income group classification were obtained from the World Bank (2018) (http://data.worldbank.org/indicator/; last accessed on December 4, 2018). To avoid the interannual inconsistent caused by income group change over time, and given that our study is for the period of 2000–2016, we used the income group classification in 2016 following previous global-scale studies (WHO, 2018; UN, 2019). National administrative boundaries were generated from the National Geographic Information Public Service Platform of China published in 2010 (http://www.tianditu.com/service/info.html?sid=1005&type=info; last accessed on December 4, 2018).

3. Methods

3.1. Determining the DSRPP areas

The DSRPP areas were designated as areas in which the annual average dust and sea-salt removed $PM_{2.5}$ concentrations were higher than the interim target one concentration (IT-1, 35 $\mu g/m^3$) according to the air quality guidelines set by the World Health Organization (WHO). We used IT-1 because it represented an achievable air quality standard for every country worldwide (WHO, 2005; Appendix Table A1). Based on the above definition, we divided the globe into DSRPP areas and non-DSRPP areas using ArcGIS 10.2 (https://www.arcgis.com/index.html).

3.2. Quantifying the spatiotemporal patterns of DSRPP

We used the landscape metrics to characterize the spatiotemporal patterns of DSRPP. A patch is a basic unit in landscape analysis, which was defined as an area differing in appearance from its surroundings (Turner and Gardner, 2015). In terms of DSRPP, a DSRPP patch refers to a continuous DSRPP area. The landscape metrics of the DSRPP can illustrate the extent, fragmentation and connectivity of DSRPP patches.

Although dozens of landscape metrics are available, most of them are highly correlated (Turner, 2015). Following previous

studies (Wu et al., 2011; Liu et al., 2017a), we chose five metrics to depict the major spatial characteristics of DSRPP. In specific, two types of most commonly used landscape metrics were applied to quantify the major spatial characteristics of DSRPP (Appendix Table A2). We used three landscape metrics to examine the basic spatial characteristics of DSRPP, including the number of patches (NP), mean patch size (MPS), and the largest patch size (LPS). NP is the number of patches in the study area, and MPS is the mean area of all the DSRPP patches, whereas LPS is the area of the largest DSRPP patch. In addition, we selected two landscape metrics, including the patch density (PD) and landscape shape index (LSI), to evaluate the structural fragmentation and geometric complexity of DSRPP. PD examines the degree of fragmentation of DSRPP patches, and LSI measures their shape complexity. All of these landscape metrics were calculated using FRAGSTATS 4.2 (McGarigal, 2015) (http://www.umass.edu/landeco/research/fragstats/fragstats.html).

Changes in landscape metrics could reveal the complex process of aggregation and fragmentation of the DSRPP patches. For example, during a process of air pollution formation, the NP of DSRPP will increase as the newly polluted patches emerge, and then decline when the patches of polluted areas further expand and aggregate. Meanwhile, the MPS and LPS of DSRPP will show an increasing trend, and the PD and LSI of DSRPP will show an inverted U shape. Otherwise, if the air quality gets improved, the polluted patches will become more fragmented at first and dissipate later, the MPS and LPS of DSRPP will decline, and the PD of DSRPP will consequently show an inverted U shape (Fig. 1).

3.3. Analyzing the spatiotemporal patterns of DSRPP on multiple scales

We analyzed the spatiotemporal patterns of DSRPP at the global and national scales. At the national scale, we mainly reported the results in China and India, because their areas of DSRPP were much larger than those in other countries. We used the linear regression (Peng et al., 2016) and Mann-Kendall test (WMO, 1991) to depict the long-term trend and significance of DSRPP from 2000 to 2016. Detailed information about the Mann-Kendall test can be found in Appendix Method A.1.

4. Results

4.1. DSRPP dynamics between 2000 and 2016 at the global scale

Overall, the global DSRPP area showed a significant increasing trend between 2000 and 2016, with the linear regression and the Mann-Kendall test passed the significance level of 0.01. The DSRPP area increased by 2,783,000 km^2 between 2000 and 2016, almost 2.5 times compared with that in 2000 (Fig. 2a, Table 1). In terms of annual dynamics, the total area of DSRPP increased from 2000 to 2008, declined slightly from 2009 to 2011, then rose again from 2012 to 2016. The total area of DSRPP reached 3,929,800 km^2 in 2016, accounting for 2.6% of the global land area (Fig. 2a; Table 1). Most increase in the area of DSRPP was concentrated in medium-income countries, which accounted for more than 90% of the growth of DSRPP area. Specifically, DSRPP area in the upper-medium and lower medium-income countries increased by 849,300 km^2 and 1,721,500 km^2, respectively, from 2000 to 2016. In addition, DSRPP area in the low income countries increased by 212,200 km^2, accounting 7.6% of the total growth (Fig. 2b).

The DSRPP became more structurally fragmented and geometrically complex over time. The NP, MPS, and LPS of DSRPP increased by 133.3%, 48.4%, and 220.5% respectively. Additionally, the PD of DSRPP increased from 0.20/million km^2 in 2000 to 0.48/million km^2 in 2016, and the LSI of DSRPP increased from 5.15 in 2000 to

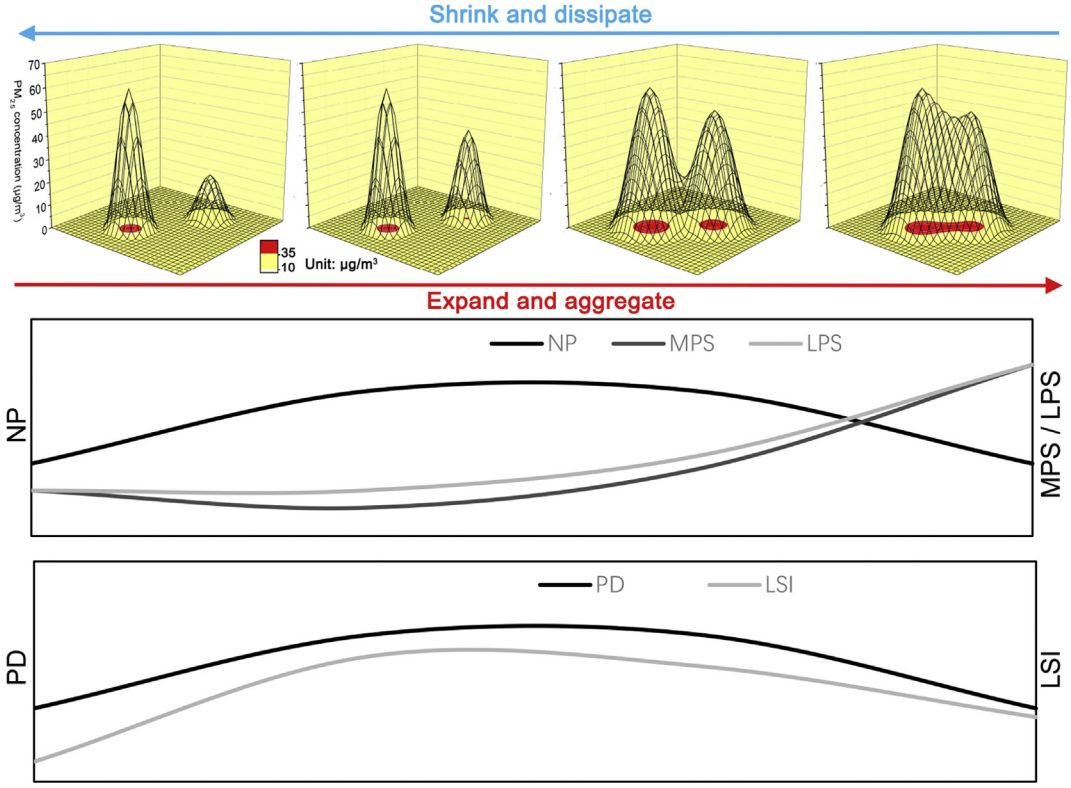

Fig. 1. Evolution of DSRPP and corresponding trends in landscape metrics.

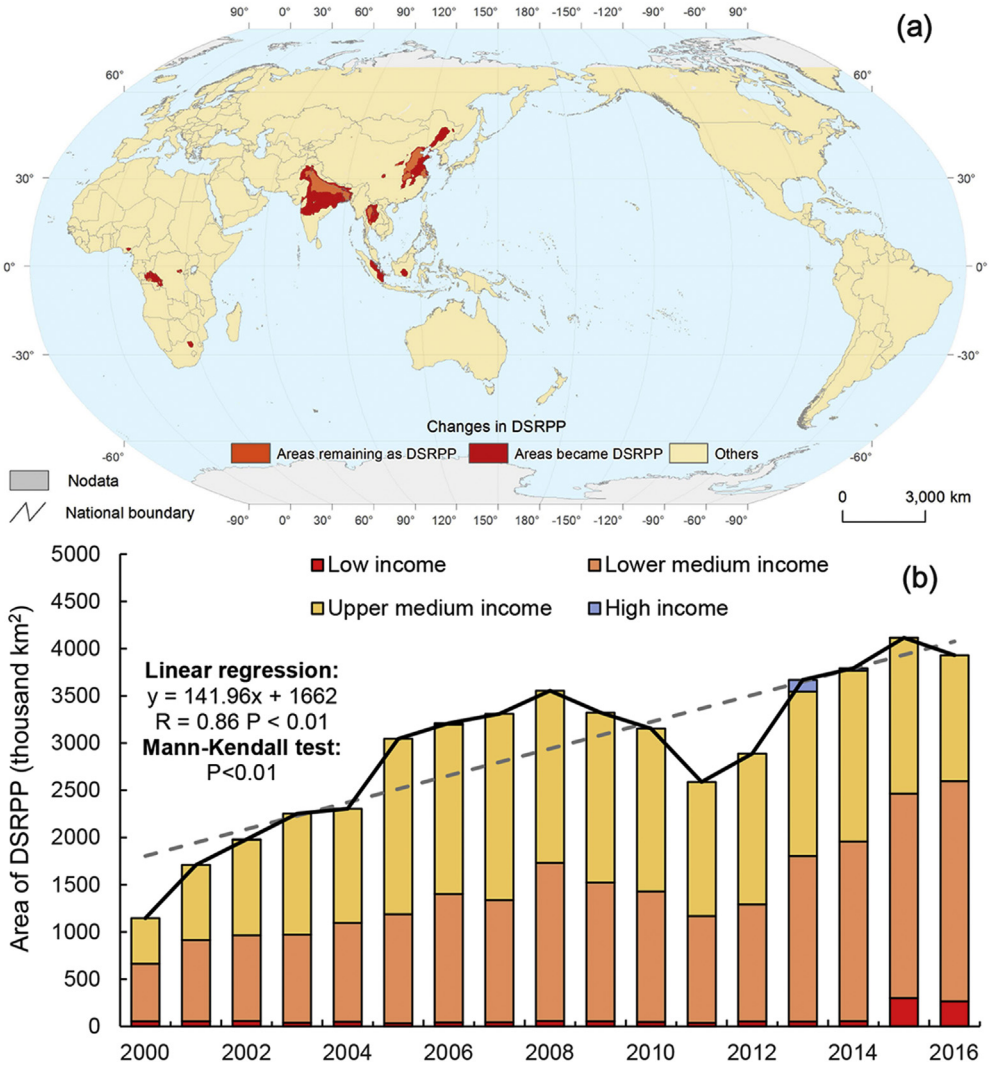

Fig. 2. Dynamics of DSRPP at the global scale.
Note: (a) Spatial changes in DSRPP between 2000 and 2016. (b) Areal changes in DSRPP from 2000 to 2016 among different income groups. The 2016 income group classification from World Bank is used in this analysis.

Table 1
Areal changes in DSRPP between 2000 and 2016.

Scale	Region	Area in 2000 (thousand km^2)	Area in 2016 (thousand km^2)	Change (thousand km^2)	Rate of change
Global	World	1,146.8	3,929.8	2,783.0	2.43
Income group	High	0.0	0.0	0.0	–
	Upper medium	484.1	1333.4	849.3	1.75
	Lower medium	608.3	2329.8	1,721.5	2.83
	Low	54.4	266.6	212.2	3.90
National	China	406.1	1,077.8	671.7	1.65
	India	490.6	1,657.6	1,167.0	2.38
	Thailand	75.6	217.6	142.0	1.88
	Bangladesh	70.9	127.7	56.8	0.80
	Pakistan	44.4	159.2	114.8	2.59
	Nepal	29.0	76.2	47.2	1.63

Note: The 2016 income group classification from World Bank is used in this analysis. For China, data do not include those from Hong Kong, China; Macao, China; and Taiwan, China for statistical purposes.

6.41 in 2016 (Fig. 3, Appendix Table A3). In terms of annual dynamics, the PD fluctuated from 2000 to 2013. During this period, the changes in DSRPP areas mainly dominated by patches in South Asia and East Asia. After the year of 2014, PD increased suddenly according to some newly added DSRPP patches in Africa and Southeast Asia. Meanwhile, the LSI of DSRPP varied from 5 to 7 from 2000 to 2016 with a moderate growth trend (Fig. 3, Appendix Figure A3).

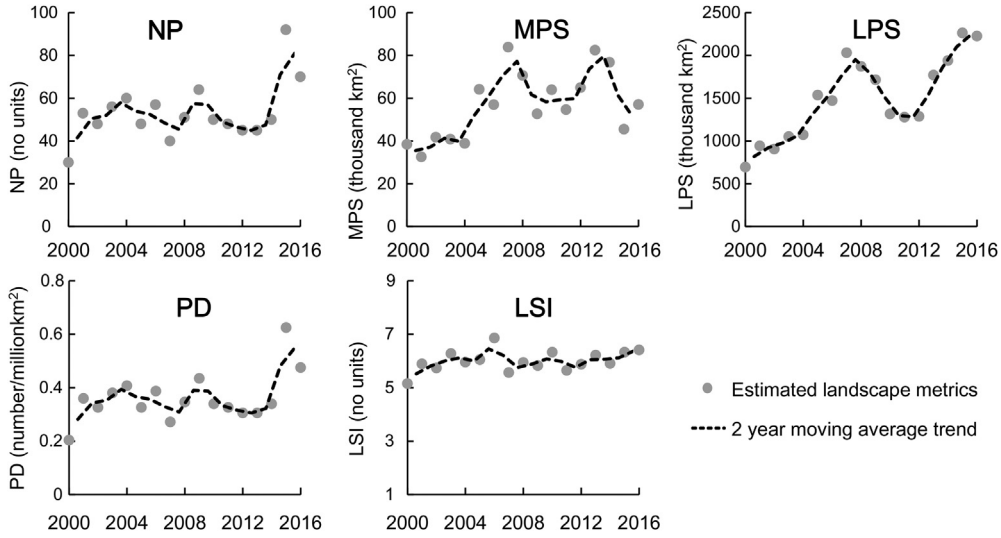

Fig. 3. Spatial patterns of DSRPP from 2000 to 2016 at the global scale.
Note: NP, number of patches; MPS, mean patch size; LPS, largest patch size; PD, patch density; LSI, landscape shape index.

4.2. DSRPP dynamics between 2000 and 2016 at the national scale

At the national scale, most of the DSRPP areas were concentrated in a few countries. The top six countries with the largest annual average DSRPP area are China, India, Thailand, Bangladesh, Pakistan and Nepal, which all belong to the medium and low income countries. The total annual average area of DSRPP in the six countries accounted for about 95% of the total DSRPP area. The DSRPP area in China and India were much larger than those in other countries, with an annual average value of 1,335,394 km^2 and 1,048,482 km^2. Correspondingly, the total areal changes in DSRPP in China and India between 2000 and 2016 reached 1,838,700 km^2, accounted for 66.1% of the total increase of DSRPP area.

4.2.1. DSRPP dynamics in China

DSRPP area in China increased by 671,700 km^2 from 2000 to 2016, accounted 1.65 times of DSRPP area in 2000. Newly added DSRPP area mainly located in the eastern region and northeastern region of China (Fig. 4a). In terms of the overall areal change, the DSRPP area in China didn't show a significant changing trend based on linear regression or Mann-Kendall test. Specifically, the DSRPP area in China increased from the year of 2000 and reached the largest area of 1,842,600 km^2 in 2007, which is about 3.5 times larger than the original area in 2000. After the year of 2007, DSRPP area experienced a declining trend, reached 1,077,800 km^2 in 2016 (Fig. 4c).

The DSRPP in China also became structurally fragmented and geometrically complex over time. The NP, MPS and LSI increased by 68.7%, 57.3% and 133.1% respectively. Along with the deterioration of air quality, existing DSRPP patches further expanded in extent and new patches of the DSRPP also appeared. These changes resulted in a 69.0% increase in the PD and a 21.3% increase in LSI of in China. In terms of annual variations, the patches of the DSRPP in China exhibited an aggregating process before 2007 and a fragmenting process after that time. Between 2000 and 2007, the MPS and LPS of the DSRPP increased by 282.1% and 419.4%, respectively. Meanwhile, the NP of the DSRPP declined from 45 in 2000 to 19 in 2007. After the year of 2007, the sizes of the DSRPP patches shrank with the values of MPS and LPS decreasing by 58.8% and 55.1%, while the NP of the DSRPP increased from 19 in 2007 to 27 in 2016 (Fig. 5; Appendix Figure A4).

4.2.2. DSRPP dynamics in India

DSRPP area in India increased by 1,167,000 km^2 from 2000 to 2016, approximately 2.38 times of that in 2000. The DSRPP areas expanded from the northern region to the central region (Fig. 4b). From the perspective of overall areal change, the areas of DSRPP in India showed an increasing trend at the significant level of 0.01 for both of the linear regression and the Mann-Kendall test, with some fluctuation from 2008 to 2012. In 2016, the areas of DSRPP in India reached 1,657,600 km^2, which is the largest among all the countries (Fig. 4c). Contrary to the recent declining trend of DSRPP in China, DSRPP area kept an increasing trend, and India ranked the first in the area of DSRPP in 2016 globally.

The DSRPP in India became more compact in structure and more complex in shape from 2000 to 2016. The NP of DSRPP decreased from 7 to 6, while the MPS and LPS increased by 294.1% and 237.4%. Some small DSRPP patches expanded and aggregated to a large DSRPP patch along with the deterioration of air quality, which lead to a small decrease in the PD of DSRPP. Meanwhile, the LSI of DSRPP increased by 17.2%, following the expansion of the DSRPP area. In terms of annual variations, the patches of the DSRPP in India showed two aggregating processes. The first aggregating period is between 2000 and 2008. In this period, the sizes of the DSRPP patches in India grew substantially with the MPS and LPS of the DSRPP patches increasing by 236.3% and 188.9%, respectively. Meanwhile, the NP of the DSRPP patches decreased from 13 in 2005 to 6 in 2008. In the second aggregating period of 2012–2016, the DSRPP patches showed a similar expanding process which is represented by increases in MPS and LPS. Consistently, the PD of the DSRPP patches during this period also increased from 9 in 2012 to 6 in 2016 (Fig. 5; Appendix Figure A5).

5. Discussion

5.1. Landscape metrics provides a new perspective to understanding the spatiotemporal patterns of air pollution

Landscape metrics were widely used to quantify the spatiotemporal characteristics of landscape elements (Turner and Gardner, 2015; Liu et al., 2017a). In this research, we used the landscape metrics to illustrate the spatiotemporal patterns of DSRPP at the global and regional scale. Our result showed that

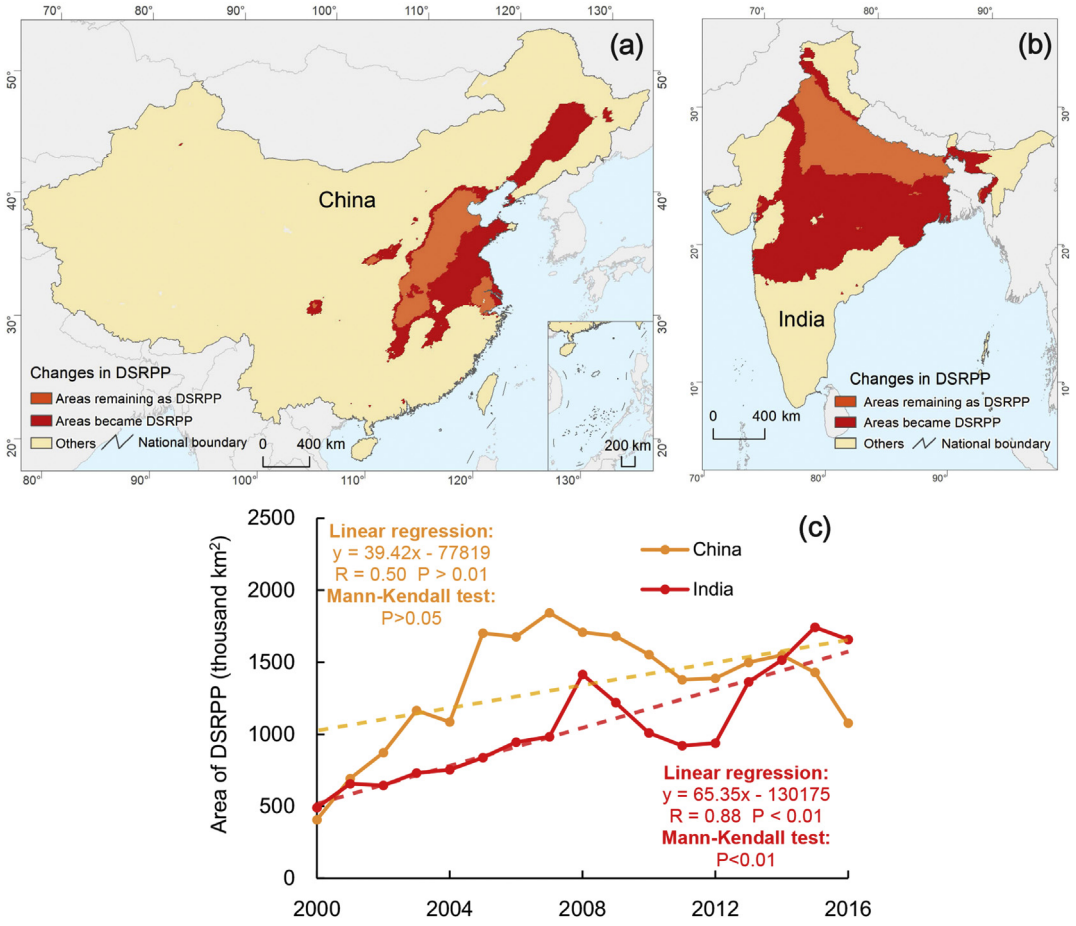

Fig. 4. Dynamics of DSRPP in China and India.
Note: (a) Spatial changes in DSRPP between 2000 and 2016 in China. (b) Spatial changes in DSRPP between 2000 and 2016 in India. (c) Areal changes in DSRPP from 2000 to 2016. For China, data do not include those from Hong Kong, China; Macao, China; and Taiwan, China for statistical purposes.

landscape metrics could identify the critical transitional stage of air quality, which provided an effective perspective to understand the evolutionary processes of DSRPP. For example, DSRPP in China deteriorated gradually from 2000 to 2007. During this period, the PD in China showed an inverted U shape, while the MPS and LPS kept growing. These changes in landscape metrics indicated that there were an expansion and aggregation of the DSRPP patches. After 2007, the area of DSRPP in China shrank in size, and the air quality got improved gradually. This transition of the spatial patterns of the DSRPP patches was in line with the decline in production-related $PM_{2.5}$ emissions in China. From 2007 to 2010, the production-related $PM_{2.5}$ emissions decreased from 9.2 million tonnes to 8.0 million tonnes (Guan et al., 2014). Besides, the promotion of large scale flue gas desulfurization also led to a reduction in air pollution (Wang et al., 2014). Between 2013 and 2016, the patches of DSRPP in China further shrank in size and some polluted patches disappeared. Therefore, the values of MPS and LPS decreased and the values of NP and PD increased. These changes also corresponded with the emissions reduction related to "China's Air Pollution Prevention and Control Action Plan" launched in 2013 (Huang et al., 2018). The plan proposes to improve air quality by reducing emissions from power plants, industrial boilers, motor vehicles and fugitive dust, with a target of lowering $PM_{2.5}$ concentration in 2017 in key regions (e.g., the Beijing-Tianjin-Hebei region) by 25% compared with 2013 (The State Council of China, 2013; Wang et al., 2017). Overall, the reduction in DSRPP is a strong evidence to indicate the great efforts in China to deal with its air pollution issues.

5.2. The relationship between areal changes in DSRPP and economic growth

The DSRPP can be influenced directly by the meteorological field and emissions of pollutants (Kaiser, 2005; West et al., 2016). The meteorological field mainly influences the transport and evolution of $PM_{2.5}$, and it is determined by multiple climatic factors such as wind speed, relative humidity and temperature (Wang et al., 2016; Yin et al., 2016). The emissions of pollutants are the sources of $PM_{2.5}$, and more closely related to anthropogenic activities such as economic activities, policy regulation and advances in technology (Gong et al., 2012; Shen et al., 2017).

The economic growth could influence the DSRPP indirectly in several different aspects. On the one hand, economic development accompanied with emissions of pollutants from multiple sources, such as industrial production, agricultural activities, and transport (Lelieveld et al., 2015; Gately et al., 2017; Zhang et al., 2017b). On the other hand, income level was also closely related to policy regulation and advances in technology, which affect the control of emission during the production processes (Guan et al., 2014; Fan et al., 2016). Following the hypothesis of the environmental Kuznets curve (EKC), environmental quality tends to get worse as economic growth occurs until the average income reaches a certain

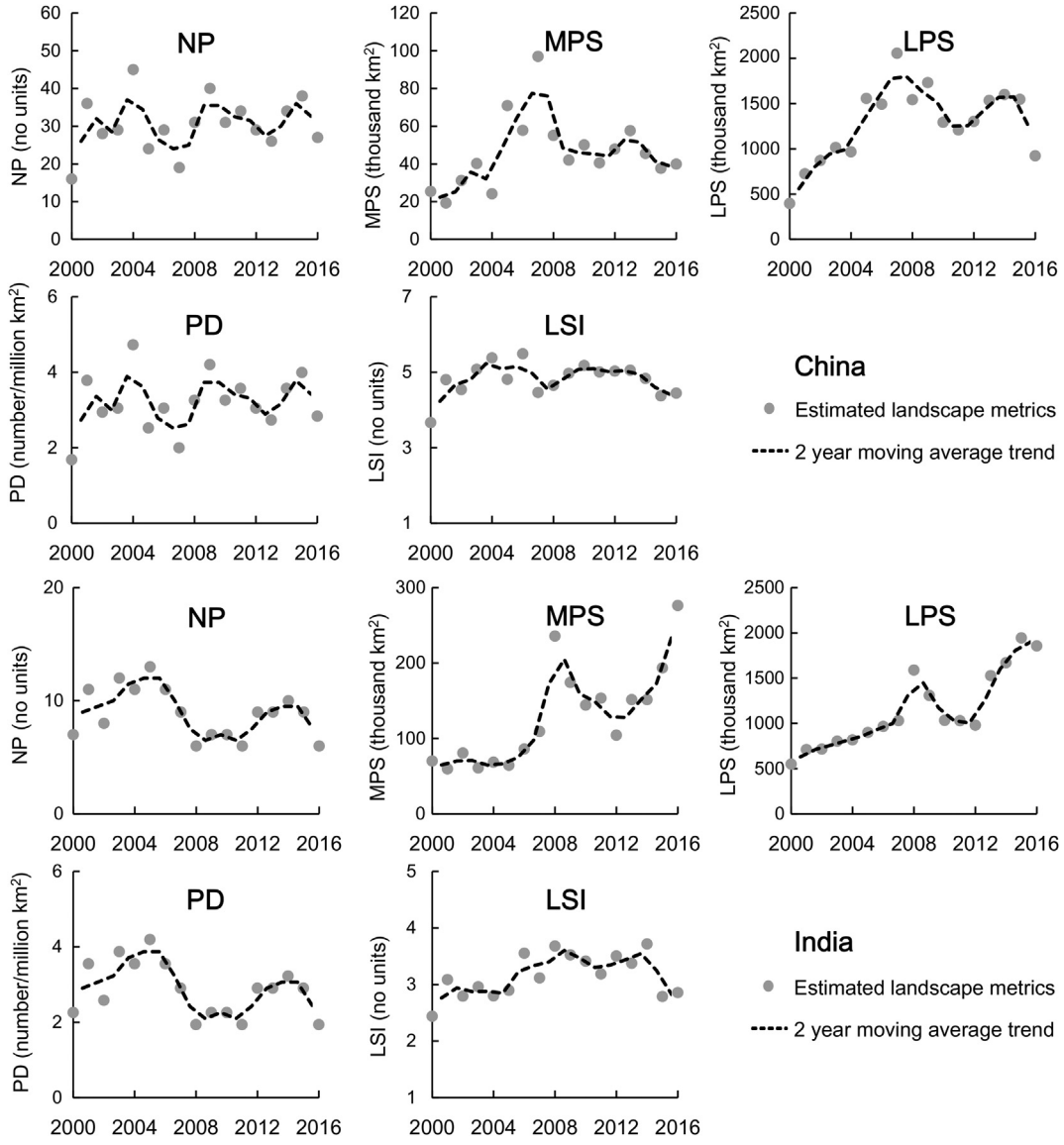

Fig. 5. Spatial patterns of DSRPP from 2000 to 2016 in China and India.
Note: NP, number of patches; MPS, mean patch size; LPS, largest patch size; PD, patch density; LSI, landscape shape index. For China, data do not include those from Hong Kong, China; Macao, China; and Taiwan, China for statistical purposes.

point with the improvement in technology and policy (Shafik, 1994). According to this framework, we compared the dynamics of DSRPP area among the four groups of countries with different income levels. The growth speed of DSRPP area decreased with the increase in income level. The change rates of DSRPP area from 2000 to 2016 were 3.90, 2.83 and 1.75 for low, lower medium and upper medium-income countries, whereas the DSRPP almost disappeared in high-income countries (Table 1). This roughly corresponded with the EKC framework.

Furthermore, we explored the relationship between economic development and the areas of DSRPP at the national scale using the element fixed effect regression model (Cheng et al., 2003; Liu et al., 2017b). The samples were collected from 12 countries, in which the areas of DSRPP were larger than zero for at least 10 years over the last. All of the 12 countries belonged to middle and low income countries. The proportion of DSRPP area to the national area and the income per capita at the national scale showed an inverse U shape. The proportion of DSRPP area in a country will increase along with the income per capita at first, and then decline after the income per capita is higher than approximately $5,000 per capita (in 2018 US dollars), which is in line with the hypothesis of EKC (Fig. 6). For the countries with an income per capita lower than the $5,000 threshold (e.g. India, Pakistan, Bangladesh and Nepal), their DSRPP areas were positively associated with income per capita. On the contrary, for countries which experienced fast economic development (e.g. China and Thailand), their DSRPP area exhibit a decreasing trend after their income per capita was greater than $ 5,000 per capita.

Our findings were also consistent with previous studies. For example, Selden and Song (1994) found that the national emissions per capita of air pollutants (i.e. SO_2, NO_X and CO) exhibited inverse U relationship with GDP per capita based on the data from 130 countries during the period of 1973–1984. Panayotou (2001) also found that ambient SO_2 level first rose, and then fell with the increase in income per capita at the national scale based on the data from 30 developed and developing countries during the period of

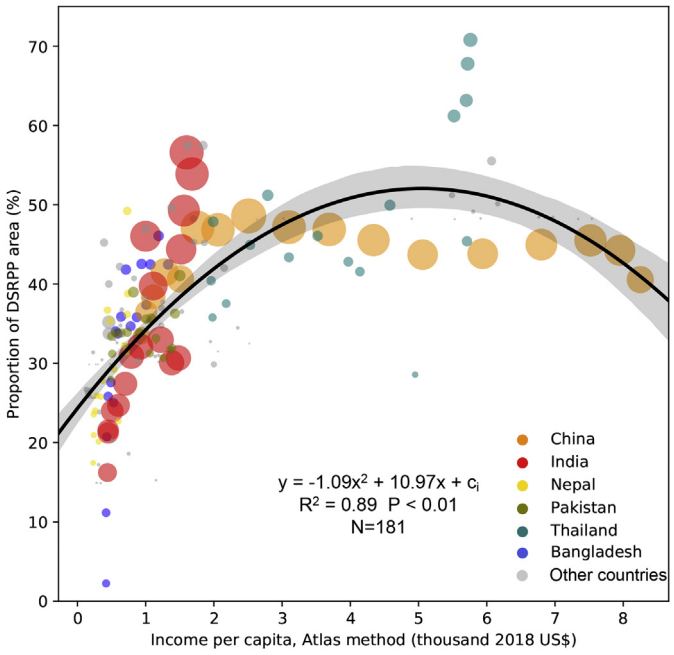

Fig. 6. Relationship between the per capita income and proportion of DSRPP area to the land area.
Note: The regression was conducted using the fixed effects model in Eviews 8. The c_i and N refer to the intercepts for different countries and the number of samples. The shaded areas and the size of the plot refer to the 95% uncertainty intervals of regression and the extents of the DSRPP area. For China, data do not include those from Hong Kong, China; Macao, China; and Taiwan, China for statistical purposes.

1982–1994. There were some differences in the turning point of the EKC between our research and previous studies. For our study, the turning point was estimated to be around $5,000 in 2018, and the estimate in a previous study was approximately $5,000 in 1984 (approximately $12,000 in 2018). The decrease in the turning point might result from the late-mover advantage suggested by previous studies, as the developing countries can learn the knowledge and technology from developed countries and avoid taking detours (Hoppe, 2000).

5.3. Mitigation of DSRPP is urgently needed to ensure the public health

DSRPP threatens human health, and people living in the DSRPP areas have higher levels of health risks. A number of studies have found that living in environments with high $PM_{2.5}$ concentrations can have various effects on human health (Kaiser, 2005; Cohen et al., 2017). Here, we used the population living in the DSRPP areas to investigate the potential human health threat posed by DSRPP, by overlaying population data and the DSRPP distribution.

The population living in DSRPP areas rapidly increased from 812.21 million in 2000 to 1,959.35 million in 2016, with a growth rate of 141.2%. At the national scale, China and India had the largest growth in the population living in DSRPP areas, accounting for 46.95% and 37.73% of the total increase at the global scale. Specifically, the population living in DSRPP in China and India increased by 367.38 million and 544.80 million, respectively, induced by the combined effects of air quality deterioration and demographic change (Appendix Figure A6). Consequently, the potential threat to public health posed by DSRPP at the global scale worsened over time.

Therefore, we argue that effective actions are required to mitigate DSRPP and protect public health in the future. Anthropogenic $PM_{2.5}$ emissions should be effectively reduced by upgrading production facilities and adjusting the energy structure (Guan et al., 2014; Huang et al., 2015). In particular, strict anthropogenic $PM_{2.5}$ emission standards should be implemented in countries with large DSRPP areas (e.g., India, China, and Thailand) (Zhao et al., 2008; Fan et al., 2016). Moreover, effective countermeasures are urgently needed to mitigate the effects of DSRPP on public health in the future. For example, healthcare in diseases associated with DSRPP should be enhanced, especially in countries with a large population living in DSRPP areas (e.g., India, China) (Guan et al., 2016; West et al., 2016).

5.4. Uncertainty analysis

In this research, we illustrated the spatiotemporal dynamics of global DSRPP from 2000 to 2016 comprehensively by combing the landscape metrics and long term global $PM_{2.5}$ concentration dataset. There are still some uncertainties in this study. First, our results are sensitive to the criteria defining the "polluted" region. In this study, we only examined the spatiotemporal patterns of DSRPP under the threshold of IT-1 (35 $\mu g/m^3$) without considering other standards. However, our findings regarding the spatiotemporal patterns of global air pollution are still notable because the IT-1 is a widely accepted threshold for determining pollution at the global scale (WHO et al., 2005; Liu et al., 2017a; Han et al., 2017b).

Second, for some regions where there is a large amount of non-anthropogenic biomass burning, the use of dust and sea-salt removed $PM_{2.5}$ as a proxy for anthropogenic $PM_{2.5}$ is not appropriate. However, this factor does not affect our major findings because the $PM_{2.5}$ pollution coming from biomass burning accounted for a small portion of $PM_{2.5}$ polluted area at the global scale (Philip et al., 2014). In addition, we did not consider the transport paths of $PM_{2.5}$ pollution as most of the $PM_{2.5}$ pollution is produced by domestic emissions (Zhang et al., 2017b).

Third, the population living in the DSRPP areas were used to roughly estimate the potential health threat posed by DSRPP. The estimates of the actual health burden attributable to DSRPP are more complex, determined by the $PM_{2.5}$ concentration, demographic factors and death rates of diseases (Cohen et al., 2017). In other words, although the area of global DSRPP increased by a factor of 2.43 from 2000 to 2016, the threats of DSRPP to public health at local scales can also decrease significantly in recent years. For example, the deaths related to $PM_{2.5}$ in China showed a decreasing trend after 2013 (Huang et al., 2018).

5.5. Application and future perspectives

Our study adapted landscape metrics to illustrate the spatiotemporal dynamics of DSRPP. Although we only used a fixed threshold and annual data in this research, this method and framework can also be adjusted to fulfill other research requests. For example, with more detailed data, landscape metrics can be powerful tools to depict the evolution process of $PM_{2.5}$ pollution at multiple spatial scales (e.g. regional and prefectural) and temporal scales (e.g. daily and monthly).

In the future, *in situ* investigations and remotely sensed data should be integrated to further quantify the spatiotemporal patterns of global air pollution. In addition, the mechanisms of the changes in DSRPP can be investigated using other methods such as atmospheric transport and dispersion models (Stein et al., 2015), emission inventory (Klimont et al., 2017) and chemical transport model (Philip et al., 2014).

6. Conclusions

The global DSRPP area rapidly increased from 1,146,800 km^2 in 2000 to 3,929,800 km^2 in 2016, with more than 90% concentrated in middle-income countries. The DSRPP became more structurally fragmented and geometrically complex during this period, with the increases in patch density and landscape shape index. Landscape metrics provided powerful tools to identify the hotspots and critical stages of air pollution at the national and regional scales. Several critical stages of DSRPP in China and India were revealed by landscape metrics effectively. Under the combined effects of air quality deterioration and demographic change, the potential threat to public health posed by air pollution increased over time, we urge that effective actions are required to mitigate the negative effects of DSRPP on public health in the future.

Author contributions

CH, QH, and HY designed the study and planned the analysis. HY did the data analysis. HY and QH drafted the manuscript. All authors contributed to the interpretation of findings, provided revisions to the manuscript, and approved the final manuscript.

Role of the funding source

The funder of the study had no role in study design, data collection, data analysis, data interpretation, or writing of the report.

Declarations of competing interest

The authors declare no competing interests.

Acknowledgments

We express our gratitude to the anonymous reviewers and editors for their professional comments and suggestions. This work was supported by the National Key R&D Program of China (Grant No. 2019YFA0607203) and the National Natural Science Foundation of China (Grant No. 41971270). It was also supported by the Second Tibetan Plateau Scientific Expedition and Research Program of China (Grant No. 2019QZKK0405) and the project from State Key Laboratory of Earth Surface Processes and Resource Ecology, China.

Appendix A. Supplementary data

Supplementary data to this article can be found online at https://doi.org/10.1016/j.jclepro.2019.119887.

References

Borrego, C., Martins, H., Tchepel, O., Salmim, L., Monteiro, A., Miranda, I., 2006. How urban structure can affect city sustainability from an air quality perspective. Environ. Model. Softw 21 (4), 461–467. https://doi.org/10.1016/j.envsoft.2004.07.009.

Burnett, R., Pope, C., Ezzati, M., Olives, C., Lim, S., Mehta, S., Shin, H., Singh, G., Hubbell, B., Brauer, M., Anderson, H., Smith, K., Balmes, J., Bruce, N., Kan, H., Laden, F., Pruess-Ustuen, A., Turner, M., Gapstur, S., Diver, W., Cohen, A., 2014. An integrated risk function for estimating the global burden of disease attributable to ambient fine particulate matter exposure. Environ. Health Perspect. 122, 397–403. https://doi.org/10.1289/ehp.1307049.

Buyantuyev, A., Wu, J., Gries, C., 2010. Multiscale analysis of the urbanization pattern of the Phoenix metropolitan landscape of USA: time, space and thematic resolution. Landsc. Urban Plan. 94 (3), 206–217. https://doi.org/10.1016/j.landurbplan.2009.10.005.

Cao, S., Zhao, W., Guan, H., Hu, D., Mo, Y., Zhao, W., Li, S., 2018. Comparison of remotely sensed $PM_{2.5}$ concentrations between developed and developing countries: results from the US, Europe, China, and India. J. Clean. Prod. 182, 672–681. https://doi.org/10.1016/j.jclepro.2018.02.096.

Cheng, H., 2003. Analysis of Panel Data. Cambridge university press, New York. https://doi.org/10.1017/CBO9780511754203.

Cheng, Z., Luo, L., Wang, S., Wang, Y., Sharma, S., Shimadera, H., Wang, X., Bressi, M., de Miranda, R., Jiang, J., Zhou, W., Fajardo, O., Yan, N., Hao, J., 2016. Status and characteristics of ambient $PM_{2.5}$ pollution in global megacities. Environ. Int. 89–90, 212–221. https://doi.org/10.1016/j.envint.2016.02.003.

Cohen, A., Brauer, M., Burnett, R., Forouzanfar, M., 2017. Estimates and 25-year trends of the global burden of disease attributable to ambient air pollution: an analysis of data from the Global Burden of Diseases Study 2015. Lancet 389, 1907–1918. https://doi.org/10.1016/s0140-6736(17)30505-6.

Crouse, D., Philip, S., van Donkelaar, A., Martin, R., Jessiman, B., Peters, P., Weichenthal, S., Brook, J., Hubbell, B., Burnett, R., 2016. A new method to jointly estimate the mortality risk of long-term exposure to fine particulate matter and its components. Sci. Rep. 6, 18916. https://doi.org/10.1038/srep18916.

Evans, J., van Donkelaar, A., Martin, R., Burnett, R., Rainham, D., Birkett, N., Krewski, D., 2013. Estimates of global mortality attributable to particulate air pollution using satellite imagery. Environ. Res. 120, 33–42. https://doi.org/10.1016/j.envres.2012.08.005.

Fan, P., Chen, J., John, R., 2016. Urbanization and environmental change during the economic transition on the Mongolian Plateau: Hohhot and Ulaanbaatar. Environ. Res. 144, 96–112. https://doi.org/10.1016/j.envres.2015.09.020. Part B.

Gately, C., Hutyra, L., Peterson, S., Wing, I., 2017. Urban emissions hotspots: quantifying vehicle congestion and air pollution using mobile phone GPS data. Environ. Pollut. 229, 496–504. https://doi.org/10.1016/j.envpol.2017.05.091.

Goldewijk, K., Beusen, A., Doelman, J., Stehfest, E., 2016. New anthropogenic land use estimates for the Holocene; HYDE 3.2. Earth Syst. Sci. Data Discuss. 1–40. https://doi.org/10.5194/essd-2016-58, 2016.

Gong, P., Liang, S., Carlton, E., Jiang, Q., Wu, J., Wang, L., Remais, J., 2012. Urbanization and health in China. The Lancet 379, 843–852. https://doi.org/10.1016/s0140-6736(11)61878-3.

Guan, D., Su, X., Zhang, Q., Glen, P., Liu, Z., Lei, Y., He, K., 2014. The socioeconomic drivers of China's primary $PM_{2.5}$ emissions. Environ. Res. Lett. 9, 024010 https://doi.org/10.1088/1748-9326/9/2/024010.

Guan, W., Zheng, X., Chung, K., Zhong, N., 2016. Impact of air pollution on the burden of chronic respiratory diseases in China: time for urgent action. The Lancet 388, 1939–1951. https://doi.org/10.1016/S0140-6736(16)31597-5.

Han, X., Liu, Y., Gao, H., Ma, J., Mao, X., Wang, Y., Ma, X., 2017a. Forecasting $PM_{2.5}$ induced male lung cancer morbidity in China using satellite retrieved $PM_{2.5}$ and spatial analysis. Sci. Total Environ. 607, 1009–1017. https://doi.org/10.1016/j.scitotenv.2017.07.061.

Han, L., Zhou, W., Li, W., Qian, Y., 2017b. Global population exposed to fine particulate pollution by population increase and pollution expansion. Air Qual. Atmos. Health 10 (10), 1–6. https://doi.org/10.1007/s11869-017-0506-8.

Hoppe, H., 2000. Second-mover advantages in the strategic adoption of new technology under uncertainty. Int. J. Ind. Organ. 18 (2), 315–338. https://doi.org/10.1016/S0167-7187(98)00020-4.

Huang, G., 2015. $PM_{2.5}$ opened a door to public participation addressing environmental challenges in China. Environ. Pollut. 197, 313–315. https://doi.org/10.1016/j.envpol.2014.12.001.

Huang, J., Pan, X., Guo, X., Li, G., 2018. Health impact of China's Air Pollution Prevention and Control Action Plan: an analysis of national air quality monitoring and mortality data. Lancet Planet. Health 2 (7), e313–e323. https://doi.org/10.1016/S2542-5196(18)30141-4.

ISO (International Organization for Standardization), 1994. Air quality-General aspects-Vocabulary. ISO4425-1994. https://www.iso.org/standard/10025.html.

Kaiser, J., 2005. Mounting evidence indicts fine-particle pollution. Science 307, 1858–1861. https://doi.org/10.1126/science.307.5717.1858a.

Klimont, Z., Kupiainen, K., Heyes, C., Purohit, P., Cofala, J., Rafaj, P., Borken-Kleefeld, J., Schöpp, W., 2017. Global anthropogenic emissions of particulate matter including black carbon. Atmos. Chem. Phys. 17, 8681–8723. https://doi.org/10.5194/acp-17-8681-2017.

Lacey, F., Marais, E., Henze, D., Lee, C., van Donkelaar, A., Martin, R., et al., 2017. Improving present day and future estimates of anthropogenic sectoral emissions and the resulting air quality impacts in Africa. Faraday Discuss 200, 397–412. https://doi.org/10.1039/c7fd00011a.

Lee, S., Hwang, S., Lee, S., Hwang, H., Sung, H., 2009. Landscape ecological approach to the relationships of land use patterns in watersheds to water quality characteristics. Landsc. Urban Plan. 92 (2), 80–89. https://doi.org/10.1016/j.landurbplan.2009.02.008.

Lelieveld, J., Evans, J., Fnais, M., Giannadaki, D., Pozzer, A., 2015. The contribution of outdoor air pollution sources to premature mortality on a global scale. Nature 525, 367–371. https://doi.org/10.1038/nature15371.

Li, G., Fang, C., Wang, S., Sun, S., 2016. The effect of economic growth, urbanization, and industrialization on fine particulate matter ($PM_{2.5}$) concentrations in China. Environ. Sci. Technol. 50 (21), 11452–11459. https://doi.org/10.1021/acs.est.6b02562.

Li, C., Martin, R., van Donkelaar, A., Boys, B., Hammer, M., Xu, J., Marais, E., Reff, A., Strum, M., Ridley, D., Crippa, M., Brauer, M., Zhang, Q., 2017. Trends in chemical composition of global and regional population-weighted fine particulate matter estimated for 25 years. Environ. Sci. Technol. 51, 11185–11195. https://doi.org/10.1021/acs.est.7b02530.

Liu, Y., Wu, J., Yu, D., 2017a. Characterizing spatiotemporal patterns of air pollution in China: a multiscale landscape approach. Ecol. Indicat. 76, 344–356. https://doi.org/10.1016/j.ecolind.2017.01.027.

Liu, M., Huang, Y., Jin, Z., Ma, Z., Liu, X., Zhang, B., Liu, Y., Yu, Y., Wang, J., Bi, J.,

Kinney, P., 2017b. The nexus between urbanization and $PM_{2.5}$ related mortality in China. Environ. Pollut. 227, 15–23. https://doi.org/10.1016/j.envint.2016.10.003.
McGarigal, K., Cushman, S., Ene, E., 2015. FRAGSTATS v4.2: Spatial Pattern Analysis Program for Categorical and Continuous Maps. Computer software program produced by the authors at the University of Massachusetts, Amherst. http://www.umass.edu/landeco/research/fragstats/downloads/fragstats_downloads.html#FRAGSTATS.
Panayotou, T., 2001. Demystifying the environmental Kuznets curve: turning a black box into a policy tool. Environ. Dev. Econ. 2, 465–484. https://doi.org/10.1017/S1355770X97000259.
Peng, J., Chen, S., Lü, H., Liu, Y., Wu, J., 2016. Spatiotemporal patterns of remotely sensed PM2.5 concentration in China from 1999 to 2011. Remote Sens. Environ. 174, 109–121. https://doi.org/10.1016/j.rse.2015.12.008.
Philip, S., Martin, R., van Donkelaar, A., Lo, J., Wang, Y., Chen, D., Zhang, L., Kasibhatla, P., Wang, S., Zhang, Q., Lu, Z., Streets, D., Bittman, S., Macdonald, D., 2014. Global chemical composition of ambient fine particulate matter for exposure assessment. Environ. Sci. Technol. 48, 13060–13068. https://doi.org/10.1021/es502965b.
Qian, Y., Zhou, W., Yu, W., Pickett, S., 2015. Quantifying spatiotemporal pattern of urban greenspace: new insights from high resolution data. Landsc. Ecol. 30 (7), 1165–1173. https://doi.org/10.1007/s10980-015-0195-3.
Remmel, T.K., Csillag, F., 2003. When are two landscape pattern indices significantly different? J. Geogr. Syst. 5 (4), 331–351. https://doi.org/10.1007/s10109-003-0116-x.
Selden, T.M., Song, D., 1994. Environmental quality and development: is there a Kuznets curve for air pollution emissions? J. Environ. Econ. Manag. 27 (2), 147–162. https://doi.org/10.1006/jeem.1994.1031.
Shafik, N., 1994. Economic development and environmental quality: an econometric analysis. Oxf. Econ. Pap. 46, 757–773. https://doi.org/10.1093/oep/46.Supplement_1.757.
Shen, H., Tao, S., Chen, Y., Ciais, P., Güneralp, B., Ru, M., Zhong, Q., Yun, X., Zhu, X., Huang, T., Tao, W., Chen, Y., Li, B., Wang, X., Liu, W., Liu, J., Zhao, S., 2017. Urbanization-induced population migration has reduced ambient $PM_{2.5}$ concentrations in China. Sci. Adv. 3 https://doi.org/10.1126/sciadv.1700300.
Stein, A., Draxler, R., Rolph, G., Stunder, B., Cohen, M., Ngan, F., 2015. NOAA's HYSPLIT atmospheric transport and dispersion modeling System. Bull. Am. Meteorol. Soc. 96 (12), 2059–2077. https://doi.org/10.1175/BAMS-D-14-00110.1.
The State Council of China, 2013. Air Pollution Prevention and Control Action Plan. http://www.gov.cn/jrzg/2013-09/12/content_2486918.htm. (Accessed 28 January 2019).
Turner, M., Gardner, R., 2015. Landscape Metrics Landscape Ecology in Theory and Practice: Pattern and Process. Springer New York, New York, NY, pp. 97–142. https://doi.org/10.1007/978-1-4939-2794-4_4.
UN (United Nations), 2019. World Population Prospects 2019. https://population.un.org/wpp/Download/Standard/Population/.
van Donkelaar, A., Martin, R., Brauer, M., Boys, B., 2015. Use of satellite observations for long-term exposure assessment of global concentrations of fine particulate matter. Environ. Health Perspect. 123 (2), 135–143. https://doi.org/10.1289/ehp.1408646.
van Donkelaar, A., Martin, R., Brauer, M., Hsu, N., Kahn, R., Levy, R., Lyapustin, A., Sayer, A., Winker, D., 2016. Global estimates of fine particulate matter using a combined geophysical-statistical method with information from satellites, Models, and Monitors. Environ. Sci. Technol. 50, 3762–3772. https://doi.org/10.1021/acs.est.5b05833.
Wang, S., Zhao, B., Cai, S., Klimont, Z., Nielsen, C.P., Morikawa, T., et al., 2014. Emission trends and mitigation options for air pollutants in East Asia. Atmos. Chem. Phys. 14 (13), 6571–6603. https://doi.org/10.5194/acp-14-6571-2014.
Wang, G., Zhang, R., Gomez, M.E., Yang, L., Levy Zamora, M., Hu, M., et al., 2016. Persistent sulfate formation from London Fog to Chinese haze. In: Proceedings of the National Academy of Sciences of the United States of America, pp. 13630–13635. https://doi.org/10.1073/pnas.1616540113.
Wang, S., Zhou, C., Wang, Z., Feng, K., Hubacek, K., 2017. The characteristics and drivers of fine particulate matter (PM2.5) distribution in China. J. Clean. Prod. 142, 1800–1809. https://doi.org/10.1016/j.jclepro.2016.11.104.
Weber, N., Haase, D., Franck, U., 2014. Assessing modelled outdoor traffic-induced noise and air pollution around urban structures using the concept of landscape metrics. Landsc. Urban Plan. 125, 105–116. https://doi.org/10.1016/j.landurbplan.2014.02.018.
West, J., Cohen, A., Dentener, F., Brunekreef, B., Zhu, T., Armstrong, B., Bell, M., Brauer, M., Carmichael, G., Costa, D., Dockery, D., Kleeman, M., Krzyzanowski, M., Kuenzli, N., Liousse, C., Lung, S., Martin, R., Poeschl, U., Pope, C., Roberts, J.M., Russell, A., Wiedinmyer, C., 2016. What we breathe impacts our health: improving understanding of the link between air pollution and health. Environ. Sci. Technol. 50, 4895–4904. https://doi.org/10.1016/j.landurbplan.2014.02.018.
WHO (World Health Organization), 2005. WHO Air Quality Guidelines for Particulate Matter, Ozone, Nitrogen Dioxide and Sulfur Dioxide. http://www.who.int/phe/health_topics/outdoorair/outdoorair_aqg/en/.
WHO (World Health Origination), 2016. Ambient Air Pollution: A Global Assessment of Exposure and Burden of Disease. http://www.who.int/phe/publications/air-pollution-global-assessment/en/.
WHO (World Health Organization), 2018. Global Health Estimates 2016: Disease Burden by Cause, Age, Sex, by Country and by Region, 2000-2016. https://www.who.int/healthinfo/global_burden_disease/estimates/en/index1.html.
WMO (World Meteorological Organization), 1991. On the Statistical Analysis of Series of Observations. http://www.wmo.int/e-catalog/detail_en.php?PUB_ID=362.
World Bank, 2018. GNI Per Capita, Atlas Method (Current US$). https://data.worldbank.org/indicator/NY.GNP.PCAP.CD?view=chart.
Wu, J., Jenerette, G.D., Buyantuyev, A., Redman, C.L., 2011. Quantifying spatiotemporal patterns of urbanization: the case of the two fastest growing metropolitan regions in the United States. Ecol. Complex. 8 (1), 1–8. https://doi.org/10.1016/j.ecocom.2010.03.002.
Wu, S., Deng, F., Hao, Y., Shima, M., Wang, X., Zheng, C., Wei, H., Lv, H., Lu, X., Huang, J., Qin, Y., Guo, X., 2013. Chemical constituents of fine particulate air pollution and pulmonary function in healthy adults: the Healthy Volunteer Natural Relocation study. J. Hazard Mater. 260, 183–191. https://doi.org/10.1016/j.jhazmat.2013.05.018.
Yin, Q., Wang, J., Hu, M., Wong, H., 2016. Estimation of daily PM2.5 concentration and its relationship with meteorological conditions in Beijing. J. Environ. Sci. 48, 161–168. https://doi.org/10.1016/j.jes.2016.03.024.
Zhang, H., Wang, Z., Zhang, W., 2016. Exploring spatiotemporal patterns of $PM_{2.5}$ in China based on ground-level observations for 190 cities. Environ. Pollut. 216, 559–567. https://doi.org/10.1016/j.envpol.2016.06.009.
Zhang, H., Hu, J., Qi, Y., Li, C., Chen, J., Wang, X., et al., 2017a. Emission characterization, environmental impact, and control measure of $PM_{2.5}$ emitted from agricultural crop residue burning in China. J. Clean. Prod. 149, 629–635. https://doi.org/10.1016/j.jclepro.2017.02.092.
Zhang, Q., Jiang, X., Tong, D., Davis, S.J., Zhao, H., Geng, G., Feng, T., Zheng, B., Lu, Z., Streets, D., Ni, R., Brauer, M., van Donkelaar, A., Martin, R., Huo, H., Liu, Z., Pan, D., Kan, H., Yan, Y., Lin, J., He, K., Guan, D., 2017b. Transboundary health impacts of transported global air pollution and international trade. Nature 543, 705–709. https://doi.org/10.1038/nature21712.
Zhao, Y., Wang, S., Duan, L., Lei, Y., Cao, P., Hao, J., 2008. Primary air pollutant emissions of coal-fired power plants in China: current status and future prediction. Atmos. Environ. 42, 8442–8452. https://doi.org/10.1016/j.atmosenv.2008.08.021.
Zhou, W., Huang, G., Cadenasso, M.L., 2011. Does spatial configuration matter? Understanding the effects of land cover pattern on land surface temperature in urban landscapes. Landsc. Urban Plan. 102 (1), 54–63. https://doi.org/10.1016/j.landurbplan.2011.03.009.